Intermolecular potential of the methane dimer and trimer

M. M. Szczęśniak, G. Chałasiński,[a] S. M. Cybulski,[b] and S. Scheiner
Department of Chemistry and Biochemistry, Southern Illinois University at Carbondale, Carbondale, Illinois 62901 and Department of Chemistry, University of Warsaw, Warsaw, Poland

The Heitler–London (HL) exchange energy is responsible for the anisotropy of the pair potential in methane. The equilibrium dimer structure is that which minimizes steric repulsion between hydrogens belonging to opposite subsystems. Dispersion energy, which represents a dominating attractive contribution, displays an orientation dependence which is the mirror image of that for HL exchange. The three-body correction to the pair potential is a superposition of HL and second-order exchange nonadditivities combined with the Axilrod–Teller dispersion nonadditivity. A great deal of cancellation between these terms results in near additivity of methane interactions in the long and intermediate regions.

I. INTRODUCTION

Interactions between methane molecules are interesting to biochemists since they represent a model for interactions in the lipid part of membranes, as well as to van der Waals chemists interested in weak intermolecular complexes. Despite its importance, no truly reliable *ab initio* potential is available for the methane–methane system as yet.

Previous *ab initio* study of the methane dimer[1] has done a credible job with the SCF part of the interaction energy. However, due to computational realities of the late seventies the correlation part was approximated by an empirical dispersion energy based upon a bond polarizability formulation. Other attempts to generate an isotropic methane–methane potential combined *ab initio* data with experimental gas-phase[2] or solid-state[3] information.

A previous SCF/STO-4G study of methane trimer,[4] on the other hand, was originally designed to pinpoint the origins of the nonadditive contributions in methane interaction. However, apart from finding that these contributions cannot be made to correlate with the induction-type nonadditivity, no conclusive evidence was presented as to their nature.

The present study is intended to apply state-of-the art methodology to generate a potential energy surface for the CH_4 dimer and to examine its components. Another objective is to elucidate the nature and magnitude of the three-body correction to the interaction in the trimer. By applying a newly proposed[5–7] combination of intermolecular Møller-Plesset perturbation theory (IMPPT)[8] with the supermolecular Møller-Plesset perturbation theory (MPPT)[9] the total interaction energy will be dissected into its contributions and the properties of each will be analyzed on an individual basis. Such an analysis will allow us to reexamine the existing potentials and to suggest ways to generate a reliable methane potential.

[a] Department of Chemistry, University of Warsaw, ul. Pasteura 1,02-093 Warsaw, Poland.
[b] Present address: Department of Chemistry, University of Ottawa, Ottawa, Ontario, K1N 6N5, Canada.

II. INTERACTION ENERGY DECOMPOSITION IN THE SUPERMOLECULAR MPPT APPROACH

The total energy of a cluster $AB...Z$ composed of subsystems $A,B,...Z$ can be defined as[10]

$$E^{(i)}{}_{AB...Z;G_{AB...Z}} = \sum_X E^{(i)}_{X;G_X} + \sum_X \tilde{\Delta} E^{(i)}_X + \sum_{X>Y} \tilde{\Delta} E^{(i)}_{XY}$$
$$+ \sum_{X>Y>W} \tilde{\Delta} E^{(i)}{}_{XYW} + \cdots + \tilde{\Delta} E^{(i)}_{AB...Z}, \quad (1)$$

where $X,Y,W = A,B,...,Z$; and (i) denotes the particular order of MPPT. The terms in Eq. (1) have clear physical interpretation. The one-body term $\tilde{\Delta} E^{(i)}{}_X$ represents the effect of the relaxation of geometry of subsystem X in the complex and is defined as

$$\tilde{\Delta} E^{(i)}_X = E^{(i)}_{X;G_{AB...Z}} - E^{(i)}_{X;G_X}, \quad (2)$$

where $E^{(i)}_{X;G_{AB...Z}}$ denotes the energy evaluated at the geometry which X assumes within complex $AB...Z$. These geometrical relaxation terms will not be considered here.

The two-body term $\tilde{\Delta} E^{(i)}_{CD}$ represents the pairwise interaction between two monomers C and D in the configuration that they assume within complex $AB...Z$:

$$\tilde{\Delta} E^{(i)}_{CD} = E^{(i)}_{CD;G_{AB...Z}} - \sum_{X=C,D} E^{(i)}_{X;G_{AB...Z}}. \quad (3)$$

Higher many-body terms are defined recursively; for example,

$$\tilde{\Delta} E^{(i)}_{CDF} = E^{(i)}_{CDF;G_{AB...Z}} - \sum_{X=C,D,} E^{(i)}_{X;G_{AB...Z}}$$
$$- \sum_{X>Y,X=C,D,F} \tilde{\Delta} E^{(i)}_{XY}. \quad (4)$$

$\tilde{\Delta} E^{(i)}_{CDF}$ represents a three-body contribution arising between relaxed-geometry monomers arranged in the same configuration as in the complex.

Decomposition of the interaction energy and interpretation of individual many-body contributions residing in Eq. (1) in terms of IMPPT is possible in light of the recent

analysis by Chałasiński *et al.*[5,6] IMPPT encompasses all well defined and meaningful contributions to the interaction energy such as electrostatic, induction, dispersion and exchange, and may be expressed in the form of a double perturbation expansion. The intermolecular interaction energy corrections $\epsilon^{(ij)}$ are of the ith order with respect to the intermolecular interaction operator and of the jth order with respect to the sum of monomer correlation potentials.

The contents of the supermolecular $\Delta E^{(i)}$ corrections will be briefly summarized below, through the third order of MPPT ($i = 3$).

A. ΔE^{SCF}

Instead of analyzing $\Delta E^{(0)}$ and $\Delta E^{(1)}$ separately it is common to consider their sum, i.e., the SCF interaction energy ΔE^{SCF}

$$\Delta E^{SCF} = \Delta E^{(0)} + \Delta E^{(1)}. \tag{5}$$

ΔE^{SCF} may be decomposed as

$$\Delta E^{SCF} = \Delta E^{HL} + \Delta E^{SCF\text{-}def}, \tag{6}$$

where ΔE^{HL} is the so called Heitler–London or Löwdin interaction energy,[11] and $\Delta E^{SCF\text{-}def}$, the SCF deformation contribution. The latter term represents effects due to relaxation of orbitals in the Coulomb field of the partner under the restriction imposed by the Pauli exclusion principle. The former, ΔE^{HL}, represents the interaction energy between mutually undeformed SCF subsystems. It may be further divided into the electrostatic, $\epsilon_{es}^{(10)}$ and exchange $\epsilon_{exch}^{(10)}$ effects, as well as "zeroth-order exchange" terms Δ_F and Δ_W of no apparent physical meaning:

$$\Delta E^{HL} = \epsilon_{es}^{(10)} + \Delta E_{exch}^{HL} = \epsilon_{es}^{(10)} + \epsilon_{exch}^{(10)} + \Delta_F + \Delta_W. \tag{7}$$

The explicit definitions of $\epsilon_{es}^{(10)}$ and $\epsilon_{exch}^{(10)}$ can be found e.g., in Ref. 11; the Δ terms were thoroughly analyzed by Gutowski *et al.*[12] Δ_F vanishes entirely if a complete basis or a basis set of the whole complex is used to describe the SCF subsystem wave functions. Δ_W is generally small compared to $\epsilon_{exch}^{(10)}$ (of the order of S^4 where S denotes the intermolecular overlap integral); it is thus convenient to combine the exchange and Δ terms together as the "HL-exchange energy," ΔE_{exch}^{HL}, as shown in Eq. (7).

It is well-known that the electrostatic term is additive.[13] Therefore, the nonadditivity of ΔE^{SCF} is determined by the nonadditivity of the HL-exchange term and the SCF-deformation contribution (cf. e.g. Refs. 14). The former is always of short-range character, i.e., decays asymptotically as $e^{-\alpha R}$.[14] The latter is determined asymptotically by the classic induction effects due to mutual electrostatic polarization of the subsystems in the complex.

It is worthwhile to note here that the method of approximation of $\Delta E^{SCF\text{-}def}$ by the effect of mutual electric polarization neglecting quantum effects of electron exchange is in practice reliable only at asymptotic distances. More importantly, however, rigorous self-consistent evaluation of polarization effects (i.e. without the Pauli principle imposed on electrons of different monomers) leads to collapse of the electrons of one monomer into the occupied orbitals of the

other.[15,16] Because of this problem we refrain from any further decomposition of $\Delta E^{SCF\text{-}def}$ into "polarization" and "charge-transfer" components.[17] Moreover, we will use the term "induction" only in reference to corrections of intermolecular perturbation theory and the energetical effect due to the induction phenomenon arising in the SCF model will be termed "deformation."

B. $\Delta E^{(2)}$

$\Delta E^{(2)}$ may be decomposed as follows:[5-7]

$$\Delta E^{(2)} = \epsilon_{es,r}^{(12)} + \epsilon_{disp}^{(20)}$$
$$+ \text{2nd-order deformation-correlation}$$
$$+ \text{2nd-order exchange-correlation}, \tag{8}$$

where $\epsilon_{es,r}^{(12)}$ denotes the second-order electrostatic-correlation energy (caused by the intramonomer correlation effect) in the "relaxed orbital" form,[7,18] and $\epsilon_{disp}^{(20)}$ is the second-order uncoupled Hartree–Fock (UCHF) dispersion energy. The second-order deformation-correlation describes the intramonomer correlation correction to the SCF-deformation contribution. In the language of perturbation theory of intermolecular forces this is the induction-correlation energy which allows for exchange effects. The rigorous decomposition of the second-order exchange term is difficult; nevertheless, we can say that it encompasses the exchange-correlation effect related to the electrostatic energy and the exchange-dispersion term. The combined second-order exchange effect can thus be approximated as follows, providing the deformation-correlation effects are negligible:[19]

$$\Delta E_{exch}^{(2)} = \Delta E^{(2)} - \epsilon_{disp}^{(20)} - \epsilon_{es,r}^{(12)}. \tag{9}$$

Some calculations of the electrostatic-correlation component were also performed in the "unrelaxed orbital" form as defined by Jeziorski *et al.*[8(b)] which is here denoted $\epsilon_{es}^{(12)}$. While the $\epsilon_{es,r}^{(12)}$ term describes asymptotically the interaction between Hartree–Fock moments of one subsystem with the second-order correlation correction to the moments described as field derivative on another, in $\epsilon_{es}^{(12)}$ the latter are described as expectation values.

Since both the electrostatic and dispersion terms in Eq. (8) are additive[13] the nonadditivity of $\Delta E^{(2)}$ is determined by the deformation-correlation and exchange correlation terms.

C. $\Delta E^{(3)}$

$\Delta E^{(3)}$ may be decomposed as follows:[5-7]

$$\Delta E^{(3)} = \epsilon_{es,r}^{(13)} + \epsilon_{disp}^{(21)} + \epsilon_{disp}^{(30)}$$
$$+ \text{3rd-order deformation-correlation}$$
$$+ \text{3rd-order exchange-correlation}, \tag{10}$$

where $\epsilon_{es,r}^{(13)}$ is the third-order electrostatic-correlation in the relaxed orbital form; $\epsilon_{disp}^{(21)}$ the first-order intramonomer-correlation correction (so-called apparent, cf. Ref. 20 and references therein) to $\epsilon_{disp}^{(20)}$, and $\epsilon_{disp}^{(30)}$ the third-order UCHF dispersion energy.

The nonadditivity of $\Delta E^{(3)}$ is thus determined by the nonadditivities of the following three components:

1. $\epsilon_{\text{disp}}^{(20)}$,

2. deformation-correlation,

3. exchange-correlation.

Due to the presence of $\epsilon_{\text{disp}}^{(30)}$, the Axilrod–Teller UCHF 3-body dispersion appears in $\Delta E^{(3)}$.[6]

To assure equality between left and right in Eqs. (5)–(10) all the perturbation terms on the right have to be derived within the dimer (trimer) centered basis sets [D(T)CBS)] and all the supermolecular quantities on the left have to be evaluated via the counterpoise procedure,[21] i.e., corrected for the basis set superposition error (BSSE).[5,6]

III. BASIS SETS AND GEOMETRIES

The calculations were performed in the "medium-polarized" basis set recently proposed by Sadlej[22] and denoted S. In this basis the polarization functions are defined as the field derivatives of the nonpolarized set and constitute two contractions of the four primitives. Despite their moderate size, $(10,6p,4d/5s,4p)$ contracted to $[5s,3p,2d/3s,2p]$ "medium-polarized" basis sets describe very well the electric properties of monomers and yield high quality interaction energies.[10,19,23] In selected dimer calculations the S basis was augmented by a single f function with the exponent 0.284^{25} and hereby denoted $S(f)$.

In the trimer calculations, however, application of the S basis would lead to 180 basis functions, too many for our computing capabilities. Therefore, in all the trimer calculations one p function on hydrogens (with the more compact exponents) was removed. Such truncation may adversely affect mainly second-order dispersion and electrostatic terms. Since, however, electrostatic energy is relatively unimportant in the CH_4 dimer, as will be shown below, and neither term contributes to nonadditive effects in the trimer, no large sacrifice of accuracy is expected due to this truncation. All the calculations were carried out using the GAUSSIAN 86[24a] program and the intermolecular perturbation theory package linked to GAUSSIAN 86.[24b]

The monomer properties of CH_4 are shown in Table I. It should be pointed out that the second-order correlation correction to the octupole moment is very sensitive to both the presence of f function and to the method of evaluation, i.e., either as an expectation value or as an analytical field derivative.

TABLE I. Monomer properties of CH_4. Octupole moment is defined as $\Omega_{xyz} = 5/2\langle\Sigma_i e_i x_i y_i z_i\rangle$, all values in a.u.

| | Basis | SCF | 2nd order correl. corrections | |
			Expect. value	Field deriv.
Ω_{xyz}[a]	S	2.1629	− 0.0103	0.0105
	$S(f)$	2.2203	0.0249	0.0583
α[b]	S	16.016		
	$S(f)$	16.029		

[a] SCF: 2.48,[25] 2.61;[24] finite field SDCI contribution: − 0.07.[26]
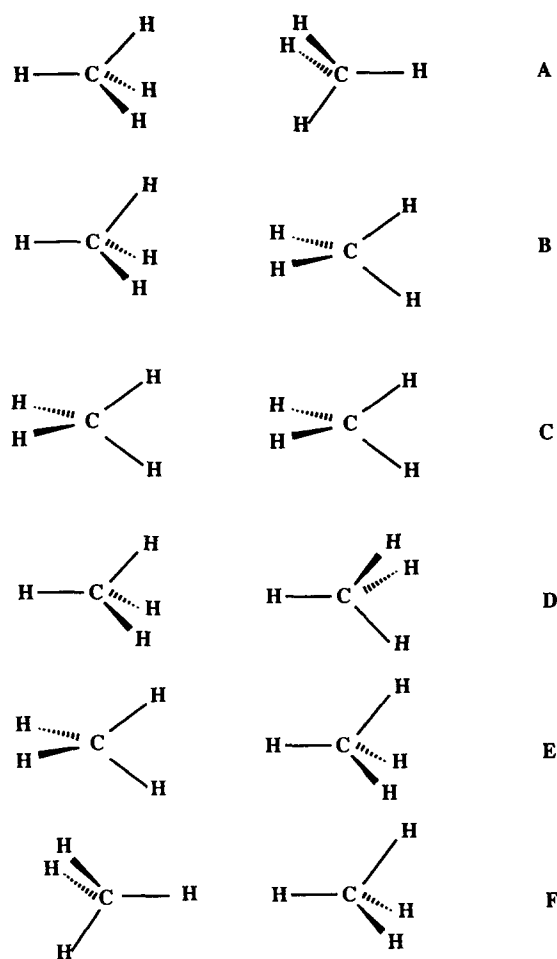[b] SCF: 16.00.[27]

FIG. 1. Six mutual orientations of the methane molecules considered in this work.

The six mutual orientations of monomers in $(CH_4)_2$, the same as in Ref. 1, are shown in Fig. 1. For example, in configuration A the two CH_4 tetrahedra are oriented so that their sides face each other. In configuration D a vertex of one faces a side of another. This is an orientation preferred by electrostatic octupole–octupole interaction. In F the two vertices face one another. The C–H bond length was equal to $2.061a_0$, the same as in Ref. 25, and R was defined as the distance between C centers.

IV. RESULTS AND DISCUSSION

A. Dimer

The equilibrium structure of $(CH_4)_2$ was found to be of type A, with $R = 7.5a_0$ at the second order MPPT. The energetic characteristics of this geometry are displayed in Table II. The interaction is repulsive at the SCF level and the major attractive contribution is due to the second-order dispersion effect, $\epsilon_{\text{disp}}^{(20)}$. The SCF interaction energy is practically unchanged upon addition of the f function. $\Delta E^{(2)}$ shows some increase presumably due to improvement in the dispersion interaction. The depth of the minimum evaluated through the second order of MPPT [$\Delta E(2)$] is equal to − 563.04 μH in the S basis and − 595.95 μH in S (f). This represents an underestimation by ~50 μH when compared to the full fourth-order MPPT [$\Delta E(4)$] treatment within the $S(f)$ ba-

TABLE II. Interaction energy of $(CH_4)_2$ in the minimum (conf. A, $R = 7.5\ a_0$) and its contributions in μH.

	SCF components		Correlation components		
	S	$S(f)$		S	$S(f)$
ΔE^{SCF}	234.96	236.24	$\Delta E^{(2)}$	-798.00	-832.19
$\epsilon_{es}^{(10)}$	-86.27		$\epsilon_{disp}^{(20)}$	-882.61	
ΔE_{exch}^{HL}	338.18		$\epsilon_{es}^{(12)}$	-22.01	
ΔE^{HL}	251.91		$\epsilon_{es,r}^{(12)}$	-30.95	
ΔE^{SCFdef}	-16.95		$\Delta E_{exch}^{(2)}$	115.56	
$\epsilon_{ind}^{(20)}$	-31.07		$\Delta E_{exch}^{(2)\sim}$	106.62	
ϵ_{ind}^{CHF}	-35.68				
$\Delta E(2)^a$	-563.04	-595.95^b			

[a] $\Delta E(n)$ represents a sum of $\Delta E^{SCF} + \Delta E^{(2)} + \cdots + \Delta E^{(n)}$.
[b] $\Delta E(4)$ for $S(f)$ basis equals -644.21.

E, μH

FIG. 2. Variation of components of the interaction energy for six orientations of the methane dimer with $R(CC) = 8a_0$.

sis set.

The repulsive nature of the SCF interaction energy results from the fact that the electrostatic attraction, $\epsilon_{es}^{(10)}$ is too weak to counteract the considerable exchange repulsion, ΔE_{exch}^{HL}. In the absence of permanent dipole and quadrupole moments the effects due to deformation of the subsystem SCF wave functions, as described by the ΔE^{SCFdef} term, are negligible. The comparison between UCHF and CHF treatments of the induction effect indicates that the CHF-induction is slightly more attractive than the UCHF. Both are quite poor approximations to the SCF-deformation effect.

The electrostatic correlation term $\epsilon_{es}^{(12)}$ is quite small. The inclusion of response effects in $\epsilon_{es,r}^{(12)}$ leads to an increase in the magnitude of electrostatic correlation by about 29%. The second-order exchange effect estimated from Eq. (9) amounts to 115.6 μH, i.e. about 30% of the HL-exchange term. A similar proportion between the HL and second-order exchange effects in the equilibrium structure was previously observed for other complexes of nonpolar systems, such as NH_3—Ar.[19] Due to the overall small magnitude of both $\epsilon_{es}^{(12)}$ and $\epsilon_{es,r}^{(12)}$ an estimate of second-order exchange may be further simplified by replacing the more costly $\epsilon_{es,r}^{(12)}$
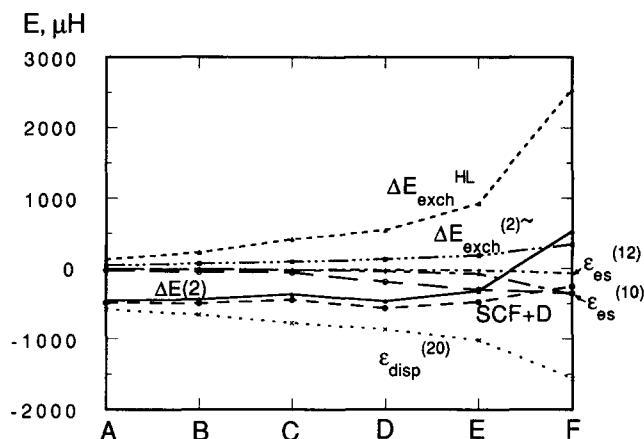
in Eq. (9) by $\epsilon_{es}^{(12)}$. The resulting quantity, denoted $\Delta E_{exch}^{(2)\sim}$ (see Table II) may serve as a satisfactory estimate of the second-order exchange effect.

In order to assess the orientation-dependence of interaction energy in the CH_4 dimer, the energy components evaluated for configurations A to F are compared at the fixed C–C distance of $8a_0$ (see Table III). As illustrated in Fig. 2, the HL-exchange contribution varies from 128 μH for A to about twenty times that for F. This is quite understandable in view of the fact that the overlap of subsystem charge distributions is minimal in the A configuration where the hydrogen atoms of the two subsystems avoid each other, and it is maximal for structure F where a pair of H atoms belonging to two subsystems are very close. Although much smaller in magnitude, $\epsilon_{es}^{(10)}$ is also quite anisotropic (attractive for all structures examined due to penetration effect). ΔE^{SCFdef} is also small and increases in magnitude monotonically from A to F. Together, they act to damp the HL-exchange energy.

The largest attractive contribution is due to the dispersion energy, $\epsilon_{disp}^{(20)}$. As is clear from Fig. 2, this term displays a behavior directly opposite to ΔE_{exch}^{HL}; namely the dispersion attraction is the weakest for A and the strongest for F. It has

TABLE III. Orientation dependence of interaction energy and its components in six configurations of $(CH_4)_2$ (see Fig. 1). $R = 8a_0$, all values in μH, basis set S.

	A	B	C	D	E	F
ΔE_{SCF}	90.69	162.65	331.20	298.37	544.11	1819.84
$\epsilon_{es}^{(10)}$	-30.21	-49.59	-58.43	-194.90	-304.54	-354.66
ΔE_{exch}^{HL}	127.90	224.53	413.92	540.15	925.40	2544.65
ΔE^{HL}	97.70	174.94	355.48	345.25	620.50	2189.99
ΔE^{SCFdef}	-7.01	-12.29	-24.29	-46.88	-76.40	-370.15
$\epsilon_{ind}^{(20)}$	-10.42	-18.98	-31.14	-59.55	-80.98	-267.24
$\Delta E^{(2)}$	-547.53	-608.24	-700.85	-767.16	-867.40	-1287.88
$\epsilon_{disp}^{(20)}$	-579.19	-660.94	-776.71	-869.33	-1022.06	-1562.82
$\epsilon_{es}^{(12)}$	-13.02	-13.98	-21.33	-26.93	-28.29	-68.19
$\Delta E_{exch}^{(2)\sim}$	44.68	66.68	97.18	129.10	182.95	343.13
$\Delta E(2)^a$	-456.84	-445.59	-369.65	-468.79	-323.29	531.96
$SCF + D^b$	-488.49	-498.30	-445.51	-570.96	-477.95	-257.02

[a] A sum of $\Delta E^{SCF} + \Delta E^{(2)}$.
[b] A sum of $\Delta E^{SCF} + \epsilon_{disp}^{(20)}$.

already been observed for several other systems[19,23,28] that the dispersion energy behaves in direct correspondence to the overlap of the subsystems' orbitals in the sense that $\epsilon_{disp}^{(20)}$ favors those orientations which allow for best overlap. However, these changes are not strong enough to counteract the even stronger variations in exchange repulsion. ΔE_{exch}^{HL} is thus the decisive factor in the anisotropy of $(CH_4)_2$. It should also be mentioned that if dispersion energy were described in an isotropic form, e.g. with the aid of an isotropic C_6 coefficient its behavior would be totally misrepresented. That is, instead of a threefold increase between A and F we would have an equal value for each of the configurations.

The anisotropic contribution to the multipole-expanded dispersion energy appears first via the C_7/R^7 term. Recent calculations of CHF dispersion coefficients through C_8 by Fowler et al.[29] allow us to compare anisotropies in both formulations of dispersion energy. First of all, the inclusion of C_7 accounts properly for the relative order of increase of dispersion attraction from A to F. However, $-C_6/R^6$-C_7/R^7 considerably underestimates the anisotropy of dispersion energy compared to our nonexpanded values. For example, at $R = 8a_0$ the difference between the values for A and F amounts to $177\,\mu H$ in the multipole formulation while our values yield a $976\,\mu H$ difference. Anisotropic components of $C_8, C_{10},...$ are unlikely to compensate for this difference.

SCF-deformation, induction, and electrostatic correlation terms do not seem important in this system. The approximate second-order exchange contribution, on the other hand, $\Delta E_{exch}^{(2)-}$ appears to be as important as $\epsilon_{es}^{(10)}$ term, or perhaps even more so. As a percent contribution of ΔE_{exch}^{HL}, the second-order exchange term varies between 49 (for A) and 19% (for F).

Upon scanning the R distance (see Table IV) the trends observed above are reinforced. Namely, the dispersion attraction increases rapidly when R decreases, and as before, in the order $A < B < C < D < E < F$ for any value of R; the exact opposite order is observed for ΔE_{exch}^{HL}. Since close approach of subsystems is prevented by even stronger increase in the exchange repulsion, the most stable configuration results from the interplay of exchange and dispersion terms. Only in structure A is the exchange repulsion weak enough so that the subsystems are allowed to approach close enough to benefit from the increase of the dispersion attraction. Despite the fact that all the other attractive contributions are the weakest here, the A configuration is the minimum energy structure for $(CH_4)_2$.

As may be seen from Table V the total interaction energy through the second-order of MPPT, $\Delta E(2)$, is negative even as close as $R = 6.5a_0$ for structure A. The global minimum occurs on the A potential energy curve at about $7.5a_0$ and its depth is some $570\,\mu H$. It is followed by a well depth of $-489\,\mu H$ for B which occurs also at $7.5a_0$. The minimum in the D curve is shifted to $8a_0(-469\,\mu H)$ and for F even

TABLE IV. Radial dependence of interaction energy for six orientations of $(CH_4)_2$. All energies in μH, R in a_0.

Configuration	R	$\epsilon_{es}^{(10)}$	ΔE_{exch}^{HL}	ΔE^{HL}	$\epsilon_{disp}^{(20)}$
A	6.0	− 1588.8	5723.3	4132.5	− 3685.2
	7.0	− 234.0	878.6	644.6	− 1382.4
	8.0	− 30.2	127.9	97.7	− 579.2
	9.0	− 2.42	16.2	13.8	− 269.6
	10.0	0.81	1.28	2.09	− 137.1
B	6.0	− 2516.7	9184.9	6668.2	− 4477.1
	7.0	− 373.2	1469.0	1095.8	− 1624.7
	8.0	− 49.6	224.5	174.9	− 660.9
	9.0	− 3.73	32.4	28.7	− 300.0
	10.0	1.36	4.31	5.67	− 149.6
C	6.0	− 3956.0	16365.5	12409.5	− 5772.5
	7.0	− 559.3	2672.8	2113.5	− 1983.0
	8.0	− 58.4	413.9	355.5	− 776.8
	9.0	4.27	60.3	64.6	− 342.1
	10.0	7.16	8.12	15.3	− 166.3
D	6.0	− 5939.3	19772.8	13833.5	− 6584.3
	7.0	− 409.7	2723.2	2313.5	− 2269.6
	8.0	− 194.9	540.1	345.2	− 869.3
	9.0	− 46.7	83.3	36.6	− 373.2
	10.0	− 16.2	12.3	− 3.85	− 177.9
E	6.0	− 9283.8	31216.4	21932.6	− 8136.3
	7.0	− 1689.1	5570.4	3881.3	− 2755.1
	8.0	− 304.5	925.0	620.5	− 1022.1
	9.0	− 63.1	144.6	81.5	− 426.0
	10.0	− 16.7	21.2	4.49	− 198.1
F	6.0	− 8686.8	83376.3	74689.5	− 14060.1
	7.0	− 2498.7	15165.3	12666.6	− 4604.4
	8.0	− 354.7	2544.7	2190.0	− 1562.8
	9.0	− 17.2	404.7	387.5	− 592.4
	10.0	15.3	61.2	76.5	− 256.2

TABLE V. Potential energy curves for four orienations of $(CH_4)_2$, in μH.

Config.	R, a_0	ΔE^{SCF}	$\Delta E^{(2)}$	$\Delta E(2)^a$	$SCF + D^b$	$HL + D^c$
A	6.0	3807.2	−2648.7	1158.5	122.0	447.3
	6.5	1523.2	−1759.2	−236.0		
	7.0	601.0	−1124.5	−523.6	−781.4	−737.8
	7.5	235.0	−798.0	−563.0	−647.7	−630.7
	8.0	90.7	−547.6	−456.8	−488.5	−481.5
	8.5	34.0	−381.3	−347.3		
	9.0	12.1	−269.5	−257.3	−257.5	−255.8
	10.0	1.51	−140.1	−138.6	−135.6	−135.0
B	6.0	6010.9	−3074.5	2936.4	1533.8	2191.1
	6.5	2484.3	−2013.5	470.8		
	7.0	1010.4	−1334.8	−324.4	−614.3	−528.9
	7.5	406.2	−895.3	−489.1		
	8.0	162.6	−608.2	−445.6	−498.3	−486.0
	9.0	26.8	−293.4	−266.6	−273.2	−271.3
	10.0	5.28	−150.2	−144.9	−144.3	−143.9
D	6.0	11440.7	−4132.9	7307.8	4856.4	7249.2
	6.5	4838.2	−2659.9	2178.3		
	7.0	1990.0	−1734.6	255.4	−279.6	43.9
	7.5	790.4	−1446.4	−356.0		
	8.0	298.4	−767.2	−468.8	−570.9	−524.1
	8.5	103.2	−520.1	−416.8		
	9.0	29.3	−357.7	−328.4	−343.9	−336.6
	10.0	−5.10	−177.2	−182.3	−183.0	−181.8
F	6.0	53429.1	−9002.1	44427.0	39369.0	60629.4
	7.0	9833.3	−3324.4	6508.9	5228.9	8062.2
	7.5	4235.0	−2050.9	2184.1		
	8.0	1819.8	−1287.9	532.0	257.0	627.2
	9.0	337.2	−542.7	−205.5	−255.2	−204.9
	10.0	69.1	−249.2	−180.0	−187.1	−179.7

[a] A sum of $\Delta E^{SCF} + \Delta E^{(2)}$.
[b] A sum of $\Delta E^{SCF} + \epsilon_{disp}^{(20)}$.
[c] A sum of $\Delta E^{HL} + \epsilon_{disp}^{(20)}$.

further, to $9a_0$ ($-205\,\mu H$). At larger R, e.g. $10a_0$ the anisotropy is controlled by the dispersion energy which dies more slowly. Still, however, the multipole expansion through C_7 predicts too isotropic a dispersion.

The question arises now as to how could the total interaction energy $\Delta E(2)$ be most easily approximated. The SCF + D column in Table V describes a total energy formulated as a sum of ΔE^{SCF} and $\epsilon_{disp}^{(20)}$. It is apparent that the SCF + D model reproduces well the potential energy surface of the CH_4 dimer. Although minima on the curves A and B are shifted toward shorter distances their proper order, i.e. A, B, D, F is correctly reproduced. Neglect of the second-order exchange repulsion, $\Delta E_{exch}^{(2)}$ in this model, makes the SCF + D curves too attractive. This is particularly noticeable at short range where the repulsive walls of the SCF + D potential are not steep enough.

Since, as pointed out above, the SCF-deformation term is not important, a further approximation is possible: i.e. replacing the ΔE^{SCF} by ΔE^{HL} in a model potential (HL + D). Due to a partial cancellation between attractive ΔE^{SCFdef} and repulsive $\Delta E_{exch}^{(2)}$ this model seems to work equally well or perhaps slightly better.

The potential energy surface of the CH_4 dimer is strongly anisotropic. For example, at $R = 7.5a_0$, where structure A has a minimum of $-563\,\mu H$ the interaction energy for F is strongly repulsive $+2184\,\mu H$. The anisotropy of the surface is determined by location of hydrogen atoms of one subsystem with respect to those of the other. If the mutual orientation of the two subsystems permits the H atoms to avoid each other the exchange repulsion is small and CH_4 molecules may approach closely, thereby allowing for better dispersion attraction. If, on the other hand, the H atoms are close to each other the exchange repulsion is large and the subsystems cannot approach too close. The presence of hydrogen atoms as the interaction sites seems to be crucial in describing the $(CH_4)_2$ potential. This is not the case in many "effective" potentials for methane which are adjusted to reproduce experimentally observed bulk properties.[30,31] An example of such a potential is the Lennard-Jones-type potential recently proposed by Jorgensen *et al.* for Monte Carlo simulations of methane.[32] Due to the fact that only C atoms are used as centers of interaction this potential is fully isotropic, i.e. the A, B, C, D, E, F configurations are represented by the same potential energy curve. The comparison of this empirical potential with the *ab initio* A, B, D, F curves is shown in Fig. 3. While the empirical potential seems to mimic the distance dependence of the D geometry quite well, it fails to resemble the others, in particular equilibrium orientation A. It should be added at this point that the fully empirical anisotropic potential for methane with C and H as explicit sites has been proposed in the past[30] and tested in molecular dynamics simulations.[33]
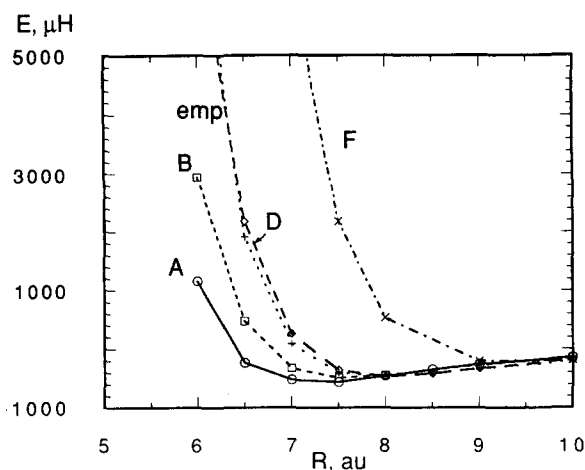
E, μH

FIG. 3. Comparison between potential energy curves for A, B, D, F structures of the methane dimer. "emp" denotes the effective potential from Ref. 32.

B. Trimer

Previous study of the three-body correction in $(CH_4)_3$ by Novaro *et al.*[4] was done only at the SCF level using the minimal STO-4G basis set. Moreover, the calculations were performed at a not too meaningful distance between C atoms equal to $4.7a_0$. Conclusions from this study are necessarily quite limited.

In the present paper the equilateral triangle geometry was chosen with a C–C distance of $7.9a_0$ which is experimentally observed in the solid.[34] The orientation of each monomer was also varied as shown in Fig. 4. R represents the intercarbon distance, and α, a deviation angle between one H atom and the C--C axis. For $\alpha = -30°$ one H atom from each CH_4 molecule points toward the center of the triangle

and for $\alpha = 95.26°$ one of the C_2 axes points in toward the center. For the latter α value calculations were also performed at $R = 10a_0$.

Prior to the truncation of the S basis set by one p-function on H atoms (the one with more compact exponents) a test dimer calculation was performed for dimer D at $R = 8a_0$. This deletion produced only a small reduction of the electrostatic and dispersion energies by 3% and 13%, respectively. The HL-exchange term remained unaffected. Neither electrostatic nor second-order dispersion components contribute to the three-body term.

The variation of the two- and three-body terms of the $(CH_4)_3$ potential as a function of the deviation angle α is shown in Table VI. As in the case of CH_4 dimer, the two-body part of the potential is dominated by the two contributions: HL-exchange and $\Delta E_{AB}^{(2)}$ whose main component is dispersion. The large values of $\widetilde{\Delta E}_{exch,AB}^{HL}$ repulsion (for $\alpha = -30°$ and $-15°$) again correspond to crowding of H atoms in the middle of the triangle. This maximal repulsion is associated with the maximal $\widetilde{\Delta E}_{AB}^{(2)}$ attraction due to the favorable dispersion energy. Electrostatic and SCF-deformation energies, although quite anisotropic, are of secondary importance; so is $\widetilde{\Delta E}_{AB}^{(3)}$.

The three-body effect is dominated by the HL-exchange term, which reaches its maximum of $-75\mu H$ at $\alpha = -30°$. $\widetilde{\Delta E}_{ABC}^{(3)}$ and $\widetilde{\Delta E}_{ABC}^{(2)}$ are smaller and of opposite sign to $\widetilde{\Delta E}_{ABC}^{HL}$. As mentioned in Sec. II $\widetilde{\Delta E}_{ABC}^{(3)}$ contains the Axilrod–Teller dispersion nonadditivity via the $\epsilon_{disp}^{(30)}$ term. Direct calculation of $\epsilon_{disp,ABC}^{(30)}$ term for $R = 10a_0$ (see last column of Table VI) yields 1.998 μH nearly identical to $\widetilde{\Delta E}_{ABC}^{(3)} = 1.99$. $\widetilde{\Delta E}_{ABC}^{(2)}$, on the other hand, should be dominated by the second-order exchange nonadditivity. Due to cancellations among all these terms the total three-body

TABLE VI. Two- and three-body contributions to the interaction energy (in μH) in equilateral CH_4 trimer.

R,a_0				7.9				10.0
α	-30	-15	0.0	20	40.53	70	95.26	95.26
				Two-body				
$\widetilde{\Delta E}_{AB}^{SCF}$	963.52	708.20	407.29	344.93	268.98	184.12	211.70	4.35
$\widetilde{\Delta E}_{AB}^{HL}$	1101.33	808.44	466.22	388.57	292.19	198.16	226.81	4.94
$\epsilon_{es,AB}^{(10)}$	-252.20	-269.59	-239.62	-185.70	-130.05	-67.53	-62.28	1.07
$\widetilde{\Delta E}_{exch,AB}^{HL}$	1353.53	1078.03	705.84	574.27	422.24	265.69	289.09	3.87
$\widetilde{\Delta E}_{AB}^{SCFdef}$	-137.81	-100.24	-58.93	-43.64	-23.21	-14.04	-15.11	-0.59
$\widetilde{\Delta E}_{AB}^{(2)}$	-831.56	-786.63	-734.47	-682.01	-613.43	-570.10	-578.94	-134.81[b]
$\widetilde{\Delta E}_{AB}^{(3)}$	-36.70	-26.79	-13.53	-12.66	-11.47	-7.90	-12.20	-1.20
$\widetilde{\Delta E}_{AB}(3)$[a]	95.26	-105.22	-340.72	-349.74	-355.93	-393.83	-379.43	-131.66
				Three-body				
$\widetilde{\Delta E}_{ABC}^{SCF}$	-74.87	-57.62	-23.34	-5.04	-1.29	-5.56	-10.36	-0.04
$\widetilde{\Delta E}_{ABC}^{HL}$	-74.89	-57.62	-22.15	-4.11	-1.46	-5.25	-9.70	-0.03
$\widetilde{\Delta E}_{ABC}^{SCFdef}$	0.02	0.0	-1.19	-0.93	0.17	-0.31	-0.66	-0.01
$\widetilde{\Delta E}_{ABC}^{(2)}$	27.28	19.17	8.79	3.94	2.79	3.69	5.10	0.06
$\widetilde{\Delta E}_{ABC}^{(3)}$	42.46	34.26	20.28	10.23	9.31	15.40	18.79	1.99[c]
$\widetilde{\Delta E}_{ABC}(3)$[a]	-5.13	-4.19	5.73	9.13	10.81	13.43	13.53	2.01
				Two- + three-body				
ΔE_{ABC}[d]	280.65	-319.85	-1016.42	-1040.08	-1056.97	-1167.96	-1124.78	-392.97

[a] Sum $\Delta E^{SCF} + \Delta E^{(2)} + \Delta E^{(3)}$.
[b] $\epsilon_{disp,AB}^{(20)} = -133.73$.
[c] $\epsilon_{disp,ABC}^{(30)} = 1.9979$.
[d] Total interaction energy of the trimer.

$\alpha = -30.0$
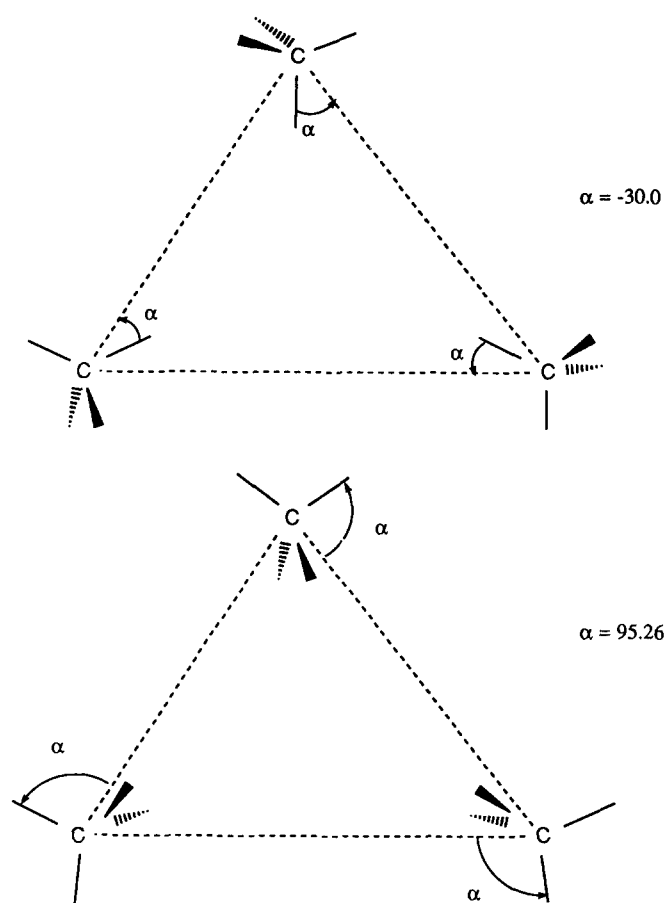
$\alpha = 95.26$

FIG. 4. Configuration of cyclic methane trimer.

FIG. 5. Various approximations to the total interaction energy ΔE_{ABC} of the cyclic $(CH_4)_3$ (solid curve). "2-" and "3-" before a symbol denote two-body and/or three-body contribution. "2-body" denotes the two-body part of the potential. ΔE_{ABC} (solid curve) and two-body (dotted curve) are nearly coincident.

term is very small, less than 2% of the total interaction energy in the trimer calculated through the third order of MPPT, ΔE_{ABC} (c.f. Table VI). Although the number of trimer configurations considered is quite limited, it is anticipated that the nonadditive effect will be quite small for geometries with larger C–C distances. Since the HL-exchange nonadditivity dies off exponentially with distance and the leading dispersion term varies asymptotically as R^{-9}, only the dispersion nonadditivity will linger as the R distance increases. For example, the calculations performed for $R = 10a_0$ (see the last column in Table VI) show that the nonadditive effect there is largely due to dispersion and constitutes only 0.5% of the full interaction energy in the trimer, ΔE_{ABC}. Therefore, around the equilibrium and at further distances, the trimer of methane may be considered pairwise additive. Consequently, in modeling of the trimer potential ΔE_{ABC} it should be enough to consider only the two-body terms. As shown in Fig. 5 the combination of the two-body HL and $\tilde{\Delta}E\,{}^{(2)}_{AB}$ terms serves this purpose very well.

It has recently been suggested that the combination of electrostatic interaction with the self-consistent polarization is capable of describing the orientation dependence of interaction energies in clusters of polar (and some nonpolar) molecules.[35] The reasoning behind this model is that the former carries most of the anisotropy of interaction while the latter accounts for nonadditive effects. It is evident from the ES + (2 + 3)-DEF curve in Fig. 5 that the application of
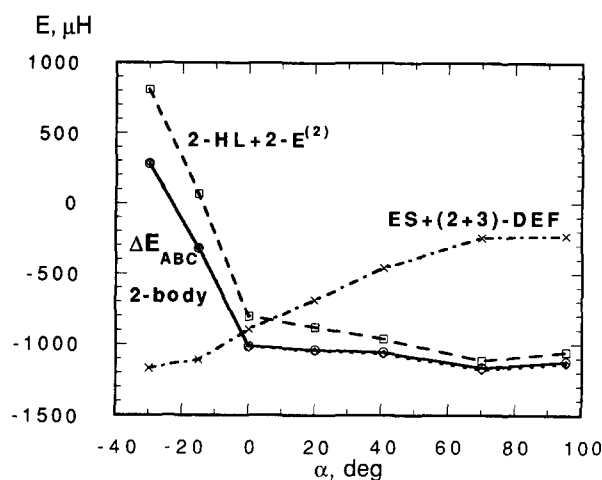
this model here by combining $\epsilon^{(10)}_{es,AB}$ with $\tilde{\Delta}E^{SCFdef}_{AB}$ and $\tilde{\Delta}E^{SCFdef}_{ABC}$ is completely unsuitable for the cluster of CH_4. First, the electrostatic term does not control the anisotropy of the interaction which is instead determined by the exchange contribution. Second, the nonadditive effect is composed of exchange (HL and second order) with Axilrod–Teller three-body dispersion, and *not* by SCF-deformation.

V. CONCLUSIONS

A. Accuracy

The potential energy surface of the methane dimer is composed largely of two competing factors: The repulsive HL-exchange effect and the dispersion attraction. The considerable anisotropy of this surface results mainly from the HL-exchange effect which in turn depends upon the relative positions of the subsystems' hydrogen atoms. It is clear that the H atoms must be included explicitly as centers of interaction in any analytical representation of the potential energy surface. The same is true of the dispersion interaction whose anisotropy matches that of exchange in the sense that the maxima in one correspond to the minima in the other.

The second-order dispersion energy is crucial to the stabilization of the methane dimer. It should thus be described as accurately as possible. The semiempirical DOSD estimate of the C_6 dispersion coefficient is 129.6 a.u.[36] The CHF calculations, on the other hand, give the value of 117.8 a.u.[29] Our calculation of $-\epsilon^{(20)}_{disp,AB} \cdot R^6$ with $\epsilon^{(20)}_{disp}$ evaluated at $R = 40a_0$ for the D configuration (in which the contribution proportional to R^7 vanishes) leads to an estimate of 120 a.u. Before any comparison is made, it should be stressed that the DOSD value corresponds to the accurate (i.e. internally correlated) dispersion energy while $\epsilon^{(20)}_{disp}$ used here is of the UCHF type. Meanwhile, our basis set underestimates dispersion interaction. The good agreement may thus be a result of some cancellation of effects of opposite sign. Due to the overall importance of dispersion energy in this system further enlargement of basis set by adding f functions on C

and d functions on H atoms are necessary. Since dispersion energy is a variational quantity in the present treatment, this could be best accomplished by optimizing the f_C and d_H exponents so as to maximize the dispersion interaction.

The three-body dispersion coefficient C_9 was estimated by a similar method as that for C_6. The calculated value $1.375^{-1} \cdot \epsilon_{\mathrm{disp},ABC}^{(30)} \cdot R^9$ with $\epsilon_{\mathrm{disp},ABC}^{(30)}$ derived at $R = 40a_0$ leads to C_9 equal to 1100 a.u. (The 1.375 is the angular factor for an equilateral triangle.) C_9 obtained in this way is considerably smaller than the DOSD value of 1631 a.u.[37] While the same factors contribute to this discrepancy as those mentioned above for C_6, it should be added that the truncation of the basis set applied in trimer calculations could adversely affect C_9.

The remaining contributions to the methane potential are quite accurate. The analysis of basis set dependence of two-body terms[7] indicates that the HL and second-order exchange, as well as deformation effects are much less basis set demanding than dispersion and are very well represented in the present basis set. The electrostatic interaction, on the other hand, is strongly basis set dependent but the basis set S was specifically designed to accurately describe this term. The same applies to the three-body part of the potential with the exception of electrostatics which does not contribute to nonadditive effects.[10,38]

The previous study of methane trimer[4] states correctly that the nonadditive component is of the same nature as in trimers of rare gas atoms such as, e.g. Ar. Indeed, our calculations[6] find in both cases that the HL- and second-order exchange effect combined with the Axilrod–Teller dispersion nonadditivity constitute the 3-body correction. The most important difference between these systems is of course the considerable anisotropy of both the 2- and 3-body potentials of methane.

Due to the cancellation among the nonadditive contributions the interaction energy of methane is pretty much pairwise additive. Thus, meaningful simulations of liquid methane are possible with a 2-body potential which at longer distances may be supplemented by the three-body dispersion term.

B. Comparison with previous anisotropic pair potentials

1. Kolos–Ranghino–Clementi–Novaro (KRCN) (Ref. 1)

In this study the interaction energy was defined as a sum of ΔE^{SCF} and anisotropic dispersion energy described in terms of empirical atom–atom parameters (bond polarizabilities and ionization energies). Two sets of data were provided for ΔE^{SCF}. The first, counterpoise corrected minimal basis set values, and second, uncorrected extended basis set data. Due to the fact that BSSE may cause serious distortions in a weak complex like methane dimer, only the first set of data is reliable. These values were compared with our ΔE^{SCF} energies. This comparison basically confirms KRCN finding as to the strong anisotropy of the SCF interaction. There are of course some slight discrepancies. For structures A, B, D, our repulsive wall of the SCF potential is slightly

less repulsive whereas it is more repulsive for F, but these differences are of the order of a few per cent.

Larger disparities are observed with dispersion energies. While their dispersion energy is capable in principle of yielding anisotropic values, their dispersion energy is far too isotropic. For example, while KRCN values agree very well with those shown in Table IV for the A geometry, their values are only half the magnitude of ours for F. One may conclude that KRCN parameters were quite well chosen despite their empirical origin. A slight reparameterization could yield very reliable values.

2. Böhm–Ahlrichs–Scharf–Schiffer (BASS) (Ref. 2)

In this model the total interaction energy ΔE is divided into a "first-order" interaction $E_{\mathrm{SCF}}^{(1)}$ and the remainder $E^{(r)}$ containing dispersion and polarization effects. The former is obtained from the probing of the Heitler–London energy between the monomer and a test system (N atom in the average-of-terms state) combined with respective combination rules and charge–charge electrostatics. The remainder in the form of damped site–site dispersion is fit to the experimental second virial coefficient. Since $E_{\mathrm{SCF}}^{(1)}$ describes approximately the Heitler–London interaction for the dimer it was thought instructive to compare these two quantities. The BASS model gives generally impressive results in the sense that the relative order of the repulsion terms for structures A through F is well reproduced. However, $E_{SCF}^{(1)}$ is systematically underestimated compared with our ΔE^{HL} (Table IV). The discrepancy is most severe for structure C where the interaction is underestimated in the repulsive region $6-8a_0$ by $\sim 20\%-25\%$.

$E^{(r)}$ was first compared with our $\epsilon_{\mathrm{disp}}^{(20)}$ as the dispersion energy is its major component. The BASS $E^{(r)}$ values are systematically more attractive than $\epsilon_{\mathrm{disp}}^{(20)}$ except for short range values in configurations E and F. The latter geometries are the regions of strong overlap and apparently the damping function of Ahlrichs, Penco, and Scoles[39] applied too strong a damping. Since $E^{(r)}$ includes also polarization effects, it may therefore be more appropriate to compare $E^{(r)}$ with our $\epsilon_{\mathrm{disp}}^{(20)} + \Delta E^{\mathrm{SCFdef}}$ or even better with $\Delta E(2)\text{-}\Delta E^{\mathrm{HL}}$ which, apart from the SCF deformation, includes also second-order exchange and other effects. The latter comparison reveals that BASS $E^{(r)}$, compared with our $\Delta E(2) - \Delta E^{\mathrm{HL}}$, is roughly 1/3 deeper for A, 1/4 for B, 1/5 for D. For structure F it is much too shallow at short range and slightly deeper at long range. It should be stressed that $E^{(r)}$ must recoup the repulsion underestimated by $E_{\mathrm{SCF}}^{(1)}$, as $E^{(r)}$ is fitted to the experimental data. On the other hand our dispersion energy, implicitly present in $\Delta E(2)$, is probably underestimated due to the fact that our basis set was truncated at d_C and p_H, and dispersion energy is of UCHF type. From the comparison we may conclude that the BASS potential is too attractive in its repulsive part and ours is probably too shallow in the minimum region. These factors apart, there is complete agreement as to the overall anisotropy of methane–methane interaction.

3. Righini–Maki–Klein (RMK) (Ref. 3)

The RMK potential combines isotropic damped dispersion energy of even powers C_6/R^6 through C_{10}/R^{10} with charge–charge electrostatics. The repulsive part is the Born–Mayer exponential term fitted to experimental solid-state data. RMK potential energy curves obtained for A, C, are nearly identical to D while F is (correctly) more repulsive. Comparing with our data the RMK potential is clearly too isotropic. First, RMK dispersion energy agrees quite well with our values for the structure D. Since, however, it is fully isotropic it remains the same for all the other structures.[40] It seems that RMK wrongly attributes the source of anisotropy of the methane–methane interaction to the electrostatic interaction. Both repulsive short-range and dispersion energy which are *de facto* strongly anisotropic, are either fully isotropic (dispersion) or nearly isotropic (Born–Mayer term) in their model. As may be seen from Table IV the electrostatic term is indeed anisotropic but its magnitude is quite small. Furthermore, we would disagree with the RMK conjecture that the overestimation of the octupole moment of methane is a cause for too high anisotropy of KRCN potential. As our results indicate, the electrostatic term in all the structures is largely due to penetration effects in the region of interest, and these effects are probably well reproduced by the KRCN basis set, as evidenced by close similarity between KRCN SCF interaction energy and ours.

As a final note, we may conclude that it is not a good idea to fit the most anisotropic part of the interaction energy to the experimental data as in the case of RMK potential. Rather one should try to obtain the anisotropy from the *ab initio* calculations and fit the more isotropic terms to the experimental data as in the strategy employed by Ahlrichs *et al.*[41] Clearly the strong anisotropy of the methane–methane potential is a fact and not an artifact of calculations.

Spherically averaged KRCN and RMK potentials (along with some effective ones) were used by Watts *et al.*[31] to analyze their scattering data. They found that the RMK gives a better representation of the scattering cross sections than the KRCN. The better performance of the RMK potential probably reflects the fact that its well depth is better represented and not the fact that the true potential is more isotropic than that of KRCN. In another scattering study Reid *et al.*[42] were unable to find a spherical form of the methane potential which fits data at both low and high collision energies together with those from the bulk. They attributed this fact to the presence of anisotropic effects which are expected to be most noticeable at the lowest collision energy. They further conclude that the spherical average of the true anisotropic potential may be significantly different from effective spherical potentials for this system.

[1] W. Kołos, G. Ranghino, E. Clementi, and O. Novaro, Int. J. Quantum Chem. **17**, 429 (1980).

[2] H. J. Böhm, R. Ahlrichs, P. Scharf, and H. Schiffer, J. Chem. Phys. **81**, 1389 (1984).

[3] (a) R. Righini, K. Maki, and M. L. Klein, Chem. Phys. Lett. **80**, 301 (1981); (b) N. Meinander and G. C. Tabisz, J. Chem. Phys. **79**, 416 (1983).

[4] O. Novaro, S. Castillo, W. Kołos, and A. Leś, Int. J. Quantum Chem. **19**, 637 (1981).

[5] G. Chałasiński and M. M. Szczęśniak, Mol. Phys. **63**, 205 (1988).

[6] G. Chałasiński, M. M. Szczęśniak, and S. M. Cybulski, J. Chem. Phys. **92**, 2481 (1990).

[7] S. M. Cybulski, G. Chałasiński, and R. Moszyński, J. Chem. Phys. **92**, 4357 (1990).

[8] (a) B. Jeziorski and W. Kołos, in *Molecular Interactions*, edited by H. Ratajczak and W. J. Orville-Thomas (Wiley, Chichester, 1982), Vol. 3; K. Szalewicz and B. Jeziorski, Mol. Phys. **38**, 191 (1979); (b) B. Jeziorski, R. Moszyński, S. Rybak, and K. Szalewicz, in *Many Body Methods in Quantum Chemistry*, edited by U. Kaldor (Springer, New York, 1989).

[9] R. J. Bartlett and D. H. Silver, Int. J. Quantum Chem. Symp. **9**, 183 (1975); J. S. Binkley and J. A. Pople, *ibid.* **9**, 227 (1975); J. A. Pople, J. S. Binkley, and R. Seeger, *ibid.* **10**, 1 (1976).

[10] G. Chałasiński, S. M. Cybulski, M. M. Szczęśniak, and S. Scheiner, J. Chem. Phys. **91**, 7048 (1989).

[11] B. Jeziorski, M. Bulski, and L. Piela, Int. J. Quantum Chem. **10**, 281 (1976).

[12] M. Gutowski, G. Chałasiński, and J. van Duijneveldt-van de Rijdt, Int. J. Quantum Chem. **26**, 971 (1984).

[13] H. Margenau and N. R. Kestner, *Theory of Intermolecular Forces*, 2nd edition (Pergamon, Oxford, 1967).

[14] W. Kołos, in *New Horizons of Quantum Chemistry*, edited by P.-O. Löwdin and B. Pullman (Reidel, Dordrecht, 1983).

[15] M. Gutowski and L. Piela, Mol. Phys. **64**, 337 (1988).

[16] R. F. Frey and E. R. Davidson, J. Chem. Phys. **90**, 555 (1989); S. M. Cybulski, and S. Scheiner, Chem. Phys. Lett. **166**, 57 (1990).

[17] K. Morokuma and K. Kitaura, in *Molecular Interactions*, edited by H. Ratajczak and W. J. Orville-Thomas (Wiley, Chichester, 1980), Vol. 1.

[18] R. Moszyński, S. Rybak, S. M. Cybulski, and G. Chałasiński, Chem. Phys. Lett. **166**, 609 (1990).

[19] G. Chałasiński, S. M. Cybulski, M. M. Szczęśniak, and S. Scheiner, J. Chem. Phys. **91**, 7809 (1989).

[20] G. Chałasiński and M. Gutowski, Chem. Rev. **88**, 943 (1988).

[21] S. F. Boys and F. Bernardi, Mol. Phys. **19**, 553 (1970).

[22] A. J. Sadlej, Coll. Czech. Chem. Commun. **53**, 1995 (1988).

[23] M. M. Szczęśniak, R. Brenstein, S. M. Cybulski, and S. Scheiner, J. Phys. Chem. **94**, 1782 (1990).

[24] (a) M. J. Frisch, J. S. Binkley, H. B. Schlegel, K. Raghavachari, C. F. Melius, R. L. Martin, J. J. P. Stewart, F. W. Bobrowicz, C. M. Rohlfing, L. R. Kahn, D. J. DeFrees, R. Seeger, R. A. Whiteside, D. J. Fox, E. M. Fluder, and J. A. Pople, GAUSSIAN 86, Carnegie-Mellon Quantum Chemistry Publishing Unit, Pittsburgh, PA, 1984; (b) S. M. Cybulski, TRURL package, 1989.

[25] G. H. F. Diercksen and A. J. Sadlej, Chem. Phys. Lett. **114**, 187 (1985).

[26] R. D. Amos, Mol. Phys. **38**, 33 (1979).

[27] H.-J. Werner and W. Meyer, Mol. Phys. **31**, 855 (1976).

[28] M. M. Szczęśniak and G. Chałasiński, Chem. Phys. Lett. **161**, 532 (1989).

[29] P. W. Fowler, P. Lazzeretti, and R. Zanasi, Mol. Phys. **68**, 853 (1989).

[30] G. C. Maitland, M. Rigby, E. B. Smith, and W. A. Wakeham, *Intermolecular Forces* (Clarendon, Oxford, 1981), p. 508.

[31] C. V. Boughton, R. E. Miller, and R. O. Watts, Mol. Phys. **56**, 363 (1985).

[32] W. L. Jorgensen, J. D. Madura, and C. J. Swenson, J. Am. Chem. Soc. **106**, 6638 (1984).

[33] S. Murad, D. J. Evans, K. E. Gubbins, W. B. Streett, and D. J. Tildeslay, Mol. Phys. **37**, 725 (1979).

[34] A. Shallamach, Proc. R. Soc. (London) A **171**, 569 (1939).

[35] C. E. Dykstra, Chem. Phys. Lett. **141**, 159 (1987); S.-Y. Liu, D. W. Michael, C. E. Dykstra, and J. M. Lisy, J. Chem. Phys. **84**, 5032 (1986).

[36] G. F. Thomas and W. J. Meath, Mol. Phys. **34**, 113 (1977).

[37] D. J. Margoliash, T. P. Proctor, G. D. Zeiss, and W. J. Meath, Mol. Phys. **35**, 747 (1978).

[38] G. Chałasiński, M. M. Szczęśniak, P. Cieplak, and S. Scheiner, J. Chem.

Phys. (submitted).

[39] R. Ahlrichs, R. Penco, and G. Scoles, Chem. Phys. **19**, 119 (1977).

[40] Meinander and Tabisz [Ref. 3(b)] attempted to add anisotropic features to RMK potential by including C_7 dispersion term.

[41] J. Hoinkis, R. Ahlrichs, and H. J. Böhm, Int. J. Quantum Chem. **23**, 821 (1983).

[42] B. P. Reid, M. J. O'Loughlin, and R. K. Sparks, J. Chem. Phys. **83**, 5656 (1985).